Molecular Dynamic Computer Simulations of Phase Behavior of Non-Ionic Surfactants

Ekaterina Ryjkina, Hubert Kuhn,* Heinz Rehage, Felix Müller, and Jörg Peggau

Surfactants, because of their varied operational possibilities, are one of the most important products for the pharmaceutical, plastic, and mineral oil industries. Research in this area plays a prominent role in interface and colloid science.

Depending on the temperature and concentration, surfactants are capable of building diverse, complex structures. The multifaceted behavior of amphiphilic substances in water in respect to aggregation activities is shown in Figure 1. At concentrations below the critical micelle concentration (cmc), surfactants tend to adsorb as a monolayer at the water–air interface. At concentrations above the cmc, they build spherical, rodlike, or disclike micelles. With further increases in the concentration of surfactant, they can occur as cubic as well as nematic, hexagonal, and lamellar mesophases. Such different aggregation forms exemplify the variety of surfactant characteristics.[1] The determination of phases and complex structures for the prediction of washing and cleaning mechanisms of surfactants with experimental methods is very important; however, the measurements of phase diagrams and the characterization of complex structures are difficult, time-consuming, and costly.

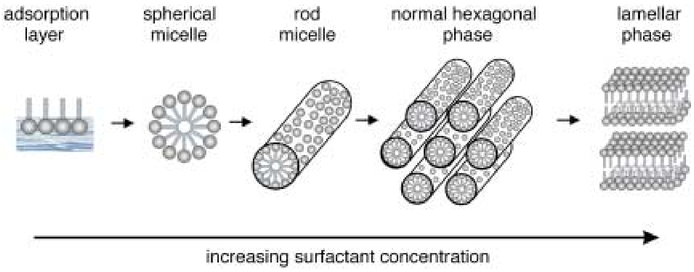

Figure 1. The building of structure and aggregation forms of surfactants in aqueous solutions depending on the surfactant concentration.

Herein, we introduce a computer simulation method that allows an easier calculation and prediction of surfactant phases in the presence of water molecules. The results for the dodecyldimethylamine oxide (DDAO; Figure 2) aqueous system presented, show that the molecular dynamics in terms of dissipative particle dynamics (DPD) can lead to an improved understanding of the structure of surfactant aggregates in water, as demonstrated by comparison of results obtained by computer simulations and experimentally determined phase diagrams of DDAO.[2]

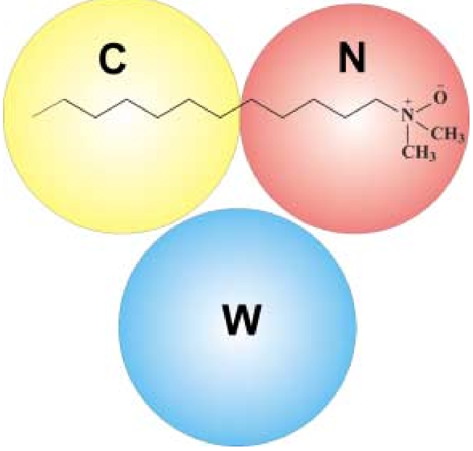

Figure 2. Schematic representation of the simulation model, which shows the fragmentation of the DDAO molecule into two DPD particles. Particles C (yellow) and N (red) are connected together with a harmonic spring. Water is treated as a separate DPD particle W (blue). The calculated repulsion parameters between particles are $a_{C-C} = a_{N-N} = a_{W-W} = 15$, $a_{N-C} = 78$, $a_{N-W} = 0$, $a_{C-W} = 80$.

The building of surfactant mesostructures with the use of classical molecular dynamic simulations at atomic resolution is currently not possible because of the time and length scales at which these phenomena can occur. To date, simulations of micelle structures at the molecular level have been restricted to isolated micelles in aqueous solution.[3]

The DPD method is a coarse-grained, mesoscale, simulation technique that was introduced by Hoogerbrugge and Koelman.[4–6] This technique allows the simulation of hydrodynamic behavior in much larger, complex systems, up to the microsecond range. The DPD simulations have been used successfully for calculations of block-copolymer microphase separation and for domain growth and phase separation in binary immiscible fluids.[7–9] The results of DPD simulations by Jury et al.[10] have shown that the phase behavior of non-ionic surfactants can be reproduced by this technique.

In DPD the fluid is modeled with soft particles (DPD particles). These particles are not regarded as the molecules of the fluid but rather as droplets or clusters of molecules. The force between each pair of particles is made of a conservative term F^C, a dissipative term F^D, and a random term F^R. The effective force F_i acting on particle i is given by Equation (1).

$$F_i = \sum_{i \neq j} F_{ij}^{C} + \sum_{i \neq j} F_{ij}^{D} + \sum_{i \neq j} F_{ij}^{R} \tag{1}$$

F^D and F^R are responsible for the conservation of total momentum in the system and incorporate the effects of Brownian motion into the larger length scale. The conservative component F^C is regarded as linear up to a cut-off radius r_c, and zero outside of this where r_{ij} is the distance between particles, e_{ij} the unity vector in the direction of the separation, and a_{ij} the interaction parameter between particles i and j [Eq. (2)]. All the forces between the DPD particles are

$$F_{ij}^{C} = \begin{cases} a_{ij}(1 - r_{ij}/r_c)e_{ij} & (r_{ij} < r_c) \\ 0 & (r_{ij} \geq r_c) \end{cases} \tag{2}$$

---

[*] Dr. H. Kuhn, E. Ryjkina, Prof. Dr. H. Rehage
Physikalische Chemie
Universität Essen
Universitätsstrasse 3–5, 45141 Essen (Germany)
Fax: (+49) 201-183-3951
E-mail: hubert.kuhn@uni-essen.de

Dr. F. Müller, J. Peggau
Degussa AG
Goldschmidtstrasse 100, 45127 Essen (Germany)

1433-7851/02/4106-0983 $ 17.50+.50/0

calculated within the constant r_c. The dissipative force F^D depends on the relative particle velocities. F^R provides the energy input in the system which together with the dissipative force, builds a thermostat. The dynamic evolution of the DPD system is governed by Newton's laws.

For the calculation of F^C, the value of a_{ij} must be determined. Here, we have obtained the interaction parameter by the calculation of mean pair contact interaction energy $\langle E_{ij}(T)\rangle$ between DPD particles, that is, between water, or hydrophilic and hydrophobic parts of the surfactant (Figure 2). In the first step, we have calculated the mixing energy of two fragments i and j $E^{ij}_{\mathrm{Mix}}(T)$ according to Equation (3).

$$E^{ij}_{\mathrm{Mix}}(T) = \frac{[Z_{ij}\langle E_{ij}(T)\rangle + Z_{ji}\langle E_{ji}(T)\rangle - Z_{ii}\langle E_{ii}(T)\rangle - Z_{jj}\langle E_{jj}(T)\rangle]}{2} \qquad (3)$$

Z_{ii}, Z_{ij}, Z_{ji}, and Z_{jj} are the calculated values of the coordination numbers for each pair of particles. The mean pair-interaction energy $\langle E_{ij}(T)\rangle$ was obtained from Monte Carlo calculations according to Equation (4).

$$\langle E_{ij}(T)\rangle = \frac{\int \mathrm{d}E_{ij}\, P(E_{ij}) E_{ij} \exp\left(\frac{-E_{ij}}{k\,T}\right)}{\int \mathrm{d}E_{ij}\, P(E_{ij}) \exp\left(\frac{-E_{ij}}{k\,T}\right)} \qquad (4)$$

$P(E_{ij})$ represents the probability distribution of pair-interaction energies. The inter and intramolecular interactions for E_{ij} calculations were calculated with the use of potential functions and parameters of the COMPASS force field. COMPASS is the most recent and accurate force field for the calculation of molecular interactions in aqueous systems. This force field is specifically parameterized for the modeling of fluids.[11, 12] The Boltzmann distribution of pair interaction energies [Eq. (3)] were generated from calculations of several thousand pairs of different molecular orientations and conformations of molecular fragments. Therefore, the pair-interaction energies were scaled with a temperature function.[13, 14] Groot and Warren have established a relationship between the Flory–Huggins interactions parameter χ and a_{ij} [Eq. (5a and b)].[15]

$$a_{ij}(T) = a_{ii} + 3.497\,\chi(T)^{ij} \qquad \text{for } \rho = 3 \qquad (5a)$$

$$a_{ij}(T) = a_{ii} + 1.451\,\chi(T)^{ij} \qquad \text{for } \rho = 5 \qquad (5b)$$

The a_{ii} terms are derived from the compressibility of pure component i ($a_{ii} = 75\,k_BT/\rho$ with density ρ).[15] For all the simulations presented here, we have set the overall particle density $\rho = N/V$ to the value 5 (in relative units, related to r_c). From the relationship between $E^{ij}_{\mathrm{Mix}}(T)$ (calculated in accordance with Equation (3)) and the Flory–Huggins parameter $\chi^{ij}(T)$ ($\chi^{ij}(T) = E^{ij}_{\mathrm{Mix}}(T)/RT$)[16] the appropriate repulsion parameter a_{ij} could be defined [Eq. (2)]. In our DPD simulations, we have used the parameters derived from Groot and Warren for the calculations of F^D_{ij} and F^R_{ij}.[15]

The amphiphilic surfactant molecule DDAO is represented by a dimeric model. The molecule is divided into two types of DPD particle, a hydrophilic particle N ($C_5H_{10}N(CH_3)_2O$) and a hydrophobic particle C(C_7H_{15}), which are connected together by a harmonic spring (Figure 2). Water molecules are represented by the monomer DPD particle W. The dynamics of 40000 DPD particles, starting from random distribution, was simulated in a cubic box under periodical boundary conditions by different surfactant concentrations. For the DPD calculations of phase structures of DDAO, different points have been chosen from an experimentally derived phase diagram,[2] at defined concentrations.[17]

Figure 3 shows the experimentally established phase diagram[2] as well as the calculated stick models (M1, H1, L1) and isodensity profiles (M2, H2, L2) of selected phase structures in thermodynamic equilibrium. The results of the calculations are in very good agreement with the experimentally observed phase structures. The isotropic micelles (M1, M2) at a surfactant concentration of $X_{\mathrm{DDAO}} = 0.5$ transform into an ordered hexagonal phase (H1, H2). By increasing the concentration of surfactant further to $X_{\mathrm{DDAO}} = 0.8$, a lamellar phase is built (L1, L2). This lamellar phase consists of double membranes comprising surfactant and water layers; the surfactant component consists of two layers of surfactant molecules, the hydrophobic groups of which are aggregated in the middle of the layer. The hydrophilic groups are oriented towards the water. In Figure 3 image L2 shows clearly the

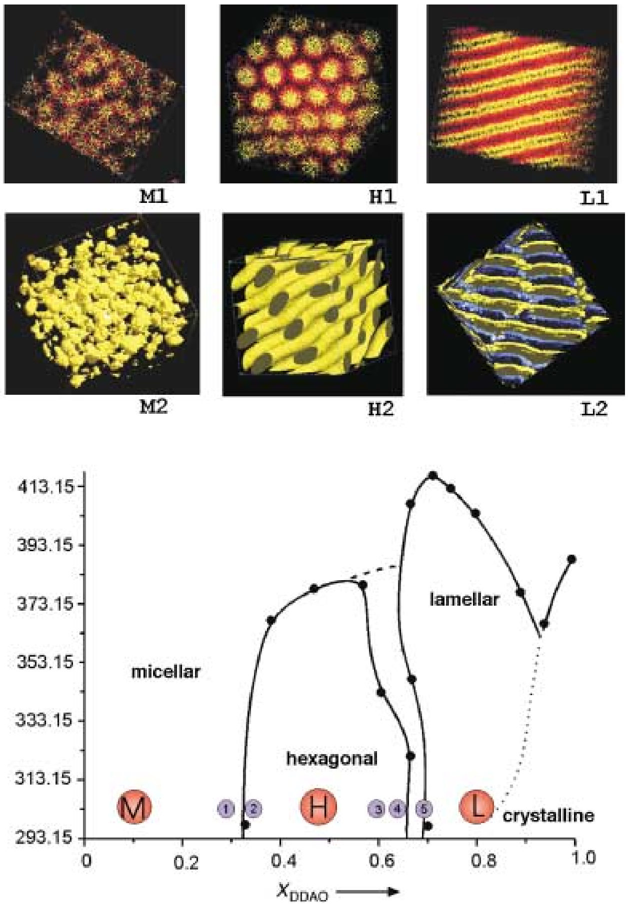

Figure 3. Experimental phase diagram of DDAO water system[2] with simulated isodensity profiles as well as the stick models of phase structures. M1, M2: micellar phase ($X_{\mathrm{DDAO}} = 0.15$, $T = 303.15$ K); H1, H2: hexagonal phase ($X_{\mathrm{DDAO}} = 0.50$, $T = 303.15$ K): L1, L2: lamella phase ($X_{\mathrm{DDAO}} = 0.80$, $T = 303.15$ K).

water layers incorporated between the lamellae. The micellar, hexagonal, and lamellar structures can be characterized well by the DPD model.

Figure 4 shows the isodensity surface as well as the stick model of DDAO at the surfactant concentration $X_{DDAO} = 0.25$ and at $T = 303.15$ K. It can be clearly shown that the concentration increase from $X_{DDAO} = 0.15$ (M1 and M2 from Figure 3) to $X_{DDAO} = 0.25$ leads to the building of a more ordered micellar phase with structured micelles.

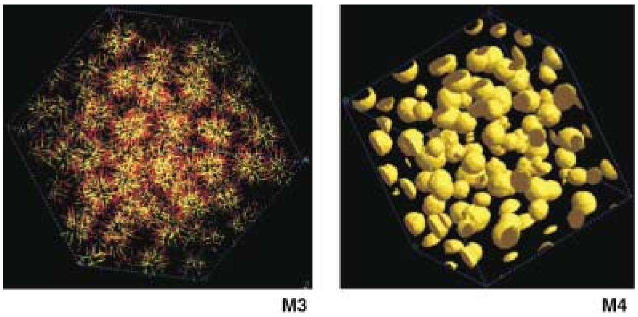

Figure 4. Representation of the micellar phase calculated with DPD at $X_{DDAO} = 0.25$ and $T = 303.15$ K.

Analysis of the isodensity profiles in sections of the simulation box at $X_{DDAO} = 0.25$ allows the calculation of the micelle aggregation number $Z_{DPD} = 71$. This calculated value is in good agreement with the small-angle neutron-scattering measurements (SANS) for DDAO above the cmc in aqueous solutions ($Z_{SANS} = 78 \pm 2$).[17]

In the hexagonal phase, highly ordered, rodlike micelles are generated. Figure 5 indicates the progressive development of the hexagonal phase during the simulation. At first a gyroid phase is formed (a, b), which during further progression of the simulation acquires a symmetry, and after 35.7 ns of total time becomes ordered in a hexagonal phase (e, f).

Additional simulations were performed at the regions of phase boundaries. All calculations were performed with $T = 303.15$ Kand for the same time range $\Delta t = 9.3$ ns (50000 time steps), but at different surfactant concentrations X_{DDAO}. The calculated concentrations are marked with blue points on the experimental phase diagram (Figure 3 ①: $X_{DDAO} = 0.30$, ②: $X_{DDAO} = 0.35$, ③: $X_{DDAO} = 0.60$, ④: $X_{DDAO} = 0.65$, ⑤: $X_{DDAO} = 0.70$). The resulting structures are presented in Figure 6. As the Figures indicate, a change in the concentration of 5% in the boundary regions between two phases can be reproduced by our DPD calculations. The spherical and rodlike micelles can be seen in Figure 6a (①). The gyroid phase in Figure 6b (②) and 6c (③) becomes ordered into a hexagonal phase during the progression of the simulation. The "viscous isotropic"[2] phase is shown in Figure 6d (④). Figure 6e and 6f show different perspectives of the structure of phase ⑤. In Figure 6e the lamellar formation can be observed, whereas in Figure 6f, the cubic formation is shown at the opposite site of the simulation box. Therefore, phase ⑤ lies in a phase coexistence region.

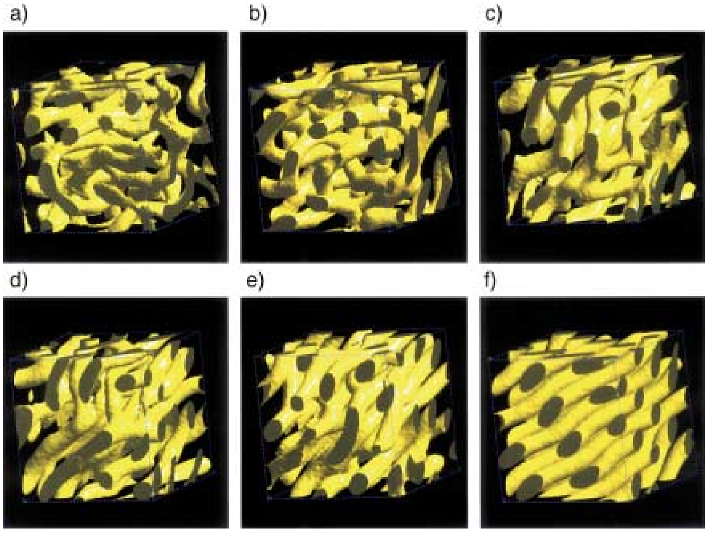

Figure 5. Calculated hexagonal phase ($X_{DDAO} = 0.50$; $T = 303.15$ K) at different simulation times a) 1.8 ns, b) 9.3 ns, c) 18.6 ns, d) 22.3 ns, e) 27.9 ns, f) 35.7 ns.

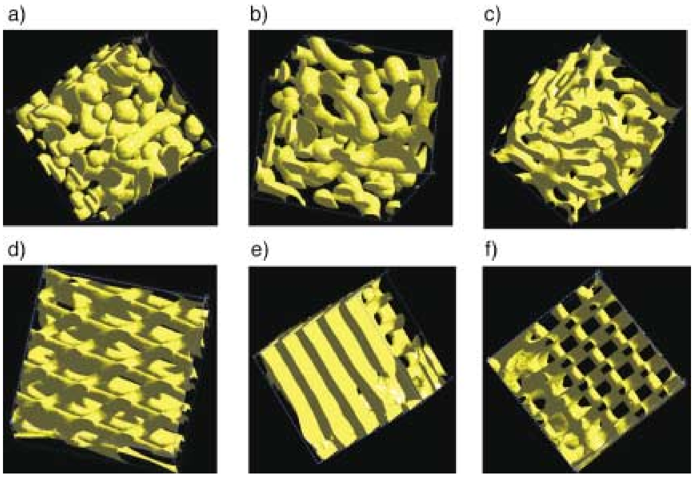

Figure 6. Representation of phase boundary regions with the DPD calculated phases at $T = 303.15$ K and surfactant concentrations: a) $X_{DDAO} = 0.30$, b) $X_{DDAO} = 0.35$, c) $X_{DDAO} = 0.60$, d) $X_{DDAO} = 0.65$, e) and f) $X_{DDAO} = 0.70$.

The DPD simulation results of a dimer model of the surfactant DDAO introduced in the present work are in very good agreement with experimentally observed phase regions. Future applications of this simulation technique could be valuable for a quick estimation of phase structures of amphiphilic molecules. The calculation effort is comparatively small, since the molecular details as well as intramolecular dynamics are not considered; however, the principal difficulty is the determination of the interaction parameters between the DPD particles.

Received: April 25, 2001
Revised: December 6, 2001 [Z16996]

---

[1] H. D. Dörfler, *Grenzflächen- und Kolloidchemie*, VCH, Weinheim, **1994**, p. 197.
[2] E. Lutton, *J. Am. Oil Chem. Soc.* **1966**, *43*, 28–30.
[3] H. Kuhn, H. Rehage, *Ber. Bunsen-Ges.* **1997**, *101*, 1485–1492.
[4] P. Hoogerbrugge, J. Koelman, *Europhys. Lett.* **1992**, *19*, 155–160.
[5] J. Koelman, P. Hoogerbrugge, *Europhys. Lett.* **1993**, *21*, 363–368.

[6] P. Espanol, P. Warren, *Europhys. Lett.* **1995**, *30*, 191–196.
[7] R. Groot, T. Madden, *J. Chem. Phys.* **1998**, *108*, 8713–8724.
[8] P. Coveney, K. Novik, *Phys. Rev. E* **1996**, *54*, 5134–5141.
[9] E. Boek, P. Coveney, H. Lekkerkerker, *J. Phys. Condens. Matter* **1996**, *8*, 9509–9512.
[10] S. Jury, P. Blandon, M. Cates, S. Krishna, M. Hagen, N. Ruddock, P. Warren, *Phys. Chem. Chem. Phys.* **1999**, *1*, 2051–2056.
[11] H. Sun, *J. Phys. Chem.* **1998**, *102*, 7338–7364.
[12] Molecular Simulations Inc., Programm Cerius2_4.1.
[13] M. Blanko, *J. Comput. Chem.* **1991**, *12*, 237–247.
[14] C. Fan, B. Olafson, M. Blanco, S. Hsu, *Macromolecules* **1992**, *25*, 3667–3676.
[15] R. Groot, P. Warren, *J. Chem. Phys.* **1997**, *107*, 4423–4435.
[16] P. Flory, *Principles of Polymer Chemistry*, Cornell University Press, Ithaca, **1953**, p. 12.
[17] V. Garamus, K. Kameyama, R. Kakehashi, H. Maeda, *Colloid Polym. Sci.* **1999**, *277*, 868–874.

A Highly Efficient Catalyst for the Telomerization of 1,3-Dienes with Alcohols: First Synthesis of a Monocarbenepalladium(0)–Olefin Complex[**]

Ralf Jackstell, Mario Gómez Andreu, Anja Frisch,
Kumaravel Selvakumar, Alexander Zapf, Holger Klein,
Anke Spannenberg, Dirk Röttger, Oliver Briel,
Ralf Karch, and Matthias Beller[*]

Dedicated to Professor Bernhard Lücke
on the occasion of his 65th birthday

Some time ago we started a program to develop atom-efficient homogeneous catalytic reactions, which are of interest for the chemical industry, especially the fine chemical industry.[1] We recently became interested in palladium-catalyzed telomerizations, since these reactions assemble simple starting materials in a 100% atom-efficient manner.[2] In general, the telomerization reaction is the dimerization of two molecules of an 1,3-diene in the presence of an appropriate nucleophile HX, for example, an alcohol,[3] to give substituted octadienes (1-substituted 2,7-octadiene, 3-substituted 1,7-octadiene). The resulting compounds are useful as intermediates in the total synthesis of several natural products[4] as well as in industry, as precursors for plasticizer alcohols,[5] monomers, solvents, corrosion inhibitors, and nonvolatile herbicides.[6]

Because of their ready availability and their exceedingly low price,[7] 1,3-butadiene and methanol are the most attractive starting materials for the telomerization reaction (Scheme 1), and yield mainly the 1-substituted 2,7-octadiene **1**. As previous studies have shown, the major by-products include the 3-substituted octa-1,7-diene (**2**; branched product), 1,3,7-octatriene (**3**; formed by the linear dimerization of butadiene), and 4-vinylcyclohexene (**4**; formed by the Diels–Alder reaction of two molecules of butadiene).

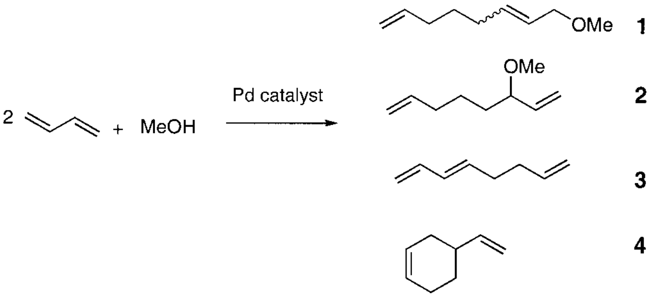

Scheme 1. Products of the telomerization of butadiene with methanol.

As a result of elegant studies from Jolly[8] and recent investigations from our side[9] the mechanism of the palladium-catalyzed telomerization reaction is well-understood. From the catalytic cycle of the reaction it is apparent that one strongly bound and sterically hindered ligand on the palladium center is sufficient to generate a productive and highly selective catalyst system. In fact, in the presence of only one strongly coordinated ligand the activity of the catalyst should be high, because free coordination sites for catalysis are readily available at the metal center.

Therefore, we had the idea that monophosphanepalladium complexes with basic phosphanes should lead to improved catalysts for telomerization reactions. Unfortunately, the tested monophosphanepalladium-1,6-diene[10] complexes proved not to be superior to the standard palladium/triphenylphosphane catalyst.[11] Next, we thought that monocarbenepalladium(0) complexes might be more suitable catalysts for our purpose. In the last five years palladium–carbene complexes have become increasingly important as catalysts for Heck-, Suzuki-, and Sonogashira reactions, copolymerizations, and aminations of aryl halides.[12] However, they have not been reported as catalysts for telomerization reactions.[13] Despite the increasing interest in this class of complexes, there are only few examples of characterized palladium(0)–carbene complexes known.[14] To our knowledge there has been no monocarbenepalladium(0) complex without additional phosphane ligands synthesized and characterized. Nevertheless, the synthesis of a monocarbenepalladium(0)–diolefin complex was achieved smoothly by treating the palladium(0)diall-

---

[*] Prof. Dr. M. Beller, Dr. R. Jackstell, Dr. M. Gómez Andreu,
Dipl.-Chem. A. Frisch, Dr. K. Selvakumar, Dr. A. Zapf,
Dipl.-Chem. H. Klein, Dr. A. Spannenberg
Institut für Organische Katalyseforschung an der
Universtität Rostock e.V. (IfOK)
Buchbinderstrasse 5–6, 18055 Rostock (Germany)
Fax: (+49) 381-4669324
E-mail: matthias.beller@ifok.uni-rostock.de
Dr. D. Röttger
Degussa AG, OXENO C4-Chemie, FEA/PS 1061/14
Paul-Baumann-Strasse 1, 45764 Marl (Germany)
Dr. O. Briel, Dr. R. Karch
OMG dmc^2 division
Rodenbacher Chaussee 4, 63403 Hanau (Germany)

[**] The work on telomerizations was supported by Degussa AG (OXENO Olefinchemie GmbH) and the synthesis of monocarbenepalladium(0) complexes was funded by OMG (former DMC^2). K.S. thanks the Alexander von Humboldt foundation for a fellowship. In addition, we thank the state of Mecklenburg-Western Pommerania for financial support. Excellent analytical service was provided by Mrs. S. Buchholz and Dr. C. Fischer (both IfOK).